MetaShield: a Multi-Function AP-Surrounding Metasurface

Burak Bilgin
Rice University
Houston, Texas, USA

Edward W. Knightly
Rice University
Houston, Texas, USA

ABSTRACT

In this work, we present MetaShield, a multi-function configurable metasurface that is affixed to and surrounds an Access Point (AP). We design MetaShield with three core features: *(i)* it is composed of configurable meta-atoms with subwavelength-scale controllable electromagnetic (EM) response, *(ii)* it provides near-field coupling with fixed geometry between the metasurface and the AP's antennas, *(iii)* it is transmissive. With these features, we design two configurations for MetaShield to undertake two functions that can be realized simultaneously in different regions of the metasurface or sequentially as dictated by the AP's protocol stack: Angle-Selective Signal Enhancement and Directional Interference Mitigation. Over-the-air experiments at 150 GHz demonstrate over 8 dB signal enhancement and 15 dB interference suppression, while supporting 20 GHz bandwidth on a single surface.

CCS CONCEPTS

• **Networks** → **Network components**; • **Hardware** → *Wireless devices*; *Networking hardware.*

1 INTRODUCTION

Next generation wireless will utilize high-frequency bands in the mmWave and sub-THz region, unlocking unprecedented bandwidth availability. Moreover, the future wireless communication environment is envisioned to be optimized according to network objectives, leading to a "smart radio environment" [1, 2]. Many recent works follow this paradigm by proposing the deployment of metasurfaces, 2D structures with subwavelength-scale amplitude and phase modulation capabilities, in the environment to provide coverage [3, 4], enable localization [5], handle polarization mismatch [6], or even implement security threats [7]. On the other hand, communication environments can and do change, leading to environment-level readjustment of such systems to continue satisfying network objectives [4]. Furthermore, each of the mentioned systems provides a single functionality, thereby requiring separate implementations to realize multiple functionalities and requiring coordination among devices to avoid unintended interactions between different systems.

In this paper, we propose MetaShield, an AP-affixed and AP-controlled multi-function configurable metasurface that conforms to and surrounds the AP in its near field, i.e., MetaShield extends the AP structure. We target millimeter wave to sub-THz bands and provide subwavelength-scale amplitude and phase control capabilities to the AP by designing MetaShield to cover a transmissive, encompassing surface with reconfigurable meta-atoms. We design MetaShield to provide multiple functionalities to the AP over its different angular regions (concurrently), and/or at different time instances (sequentially). Furthermore, we design three meta-atom configurations that leverage the near-field, fixed location of MetaShield relative to the AP to provide the three following functionalities.

1 - Random Blocks Configuration for One Shot Angular Localization. We exploit the subwavelength-scale EM manipulation capability of MetaShield by randomly configuring its meta-atoms in a blockwise fashion to realize angle-specific spectral signatures to be observed by the AP. Thus, during directional link establishment or client or environmental mobility, the AP uses this configuration on MetaShield to angularly localize the client via pre-defined signatures in a "one-shot" manner, eliminating the need for a high-overhead sequential beam sweep. Due to space limits, the design and experimental analysis of this functionality is not included in this paper, and can be found in [8].

2- MetaShield-to-AP Focus Configuration for Angle-Selective Signal Enhancement. We leverage the affixed position of MetaShield in the near-field of the AP to design a meta-atom configuration that focuses incoming EM waves impinging on MetaShield onto the AP's aperture to provide

ACM WiNTECH' 23, October 6, 2023, Madrid, Spain

ACM ISBN 979-8-4007-0340-9/23/10…$15.00
https://doi.org/10.1145/3615453.3616510

maximal signal power. Unlike prior metasurface-based focusing solutions that are typically implemented in the environment, MetaShield can provide the AP with an "acceptance window", i.e., the AP can determine the specific angular region of MetaShield to focus the incident beam from based on the intended user location, minimizing interference leakage.

3- Single-Mode Resonance Configuration for Directional Interference Mitigation. We utilize the resonance nature of meta-atoms and design a configuration that directionally prohibits EM waves from passing through MetaShield by maximally absorbing EM energy at the desired resonance frequency band. By using this configuration concurrently with the Focuser Configuration over different regions of MetaShield, the AP can block signals coming from unintended sources and enhance the intended signal power at the same time, without implementing separate systems.

We fabricate each of these designed configurations both individually in a planar structure, as well as jointly in a cylindrical conforming structure (the analysis for angular localization and conformal structure can be found in [8]). We experimentally analyze MetaShield by performing over-the-air experiments with a Time-domain Spectroscopy (TDS) system over a wide sub-THz bandwidth and have the following exemplary findings: First, the Single-Mode Resonance Configuration realizes up to 15 dB signal suppression while supporting a 20 GHz bandwidth having over 9 dB suppression at a wide range of signal reception angles. Second, the Focuser Configuration achieves over 8 dB SNR gain at the 150 GHz center frequency, and demonstrates wide band focusing, showing its effectiveness for wideband sub-THz links.

The related work addressing MetaShield's targeted functionalities in the mmWave to sub-THz bands can be categorized into the following fields:

Interference Management. Prior interference mitigation solutions include beamforming schemes, e.g. [9, 10], which require interferer localization, and are therefore ineffective against non-cooperating interferers. While [11, 12] provide methods that mitigate interference from non-cooperating users, they work in restricted environments, or against limited interference profiles. In contrast, MetaShield provides interference mitigation to the AP without any interferer location or environment-based knowledge, and is configured based on the intended user's location only, which is an underlying protocol requirement for link establishment.

Focusing. Recent works have realized beam focusing metasurfaces [3, 13–19], where the metasurface is usually proposed to be integrated into the environment for signal enhancement. Unlike the listed works, MetaShield does not require distance estimation prior to focusing onto the AP's aperture due to its AP-affixed architecture, which also provides the AP with Angle-Selective Focusing, i.e., the capability of selecting a focusing window, and blocking the signals received from the rest of the environment with Single-Mode Resonance Configuration.

Metasurface enhanced networks. Future networks promise the use of metasurfaces for high-resolution manipulation of wireless channels, e.g., [1–7, 12]. The common goal of these works is to manipulate the propagation environment by providing coverage, localization, polarization control etc. via implementing metasurfaces in the environment, i.e., on walls, windows or other structural elements [3–7, 12]. In contrast, we propose an *AP-affixed metasurface*, and provide multiple functionalities to an AP over a single surface with MetaShield. By doing so, we devise the first architecture to realize multiple concurrent and configurable functions, thereby eliminating the need to coordinate and control interactions among multiple single-function devices.

2 METASHIELD ARCHITECTURE

In this section, we describe the MetaShield architecture and two exemplary functions that can be realized via meta-atom configurations described in Section 3.

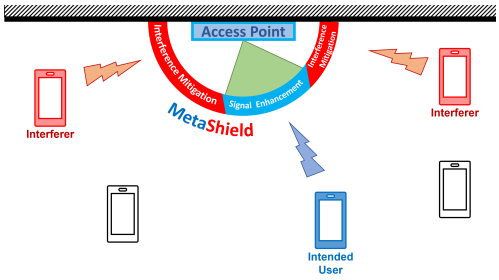

Figure 1: MetaShield architecture.

Transmissive and Conformal Structure. MetaShield is a transmissive metasurface that surrounds an AP to transform electromagnetic wavefronts as they pass through the surface, enclosing the AP on all transmitting and receiving sides as illustrated in Figure 1. For example, a ceiling-mounted AP provides downward coverage in all directions, and in this case, MetaShield surrounds the AP below it and to its sides, thereby enabling MetaShield to modulate signals arriving from all directions served by the AP.

Multi-Functional. The conformal structure not only provides full angular coverage, but also enables MetaShield to spatially distribute multiple functionalities to different regions over its surface, thus enabling concurrent functionality. In this paper, we design and implement two functionalities:

(1) Directional signal enhancement via beam focusing with a lens-like phase modulation. Once the intended user is localized, traditional methods employ receive beam forming to enhance the signal at the receiver. In contrast, because MetaShield is in the near field of the AP and has a fixed and known geometry between MetaShield and the AP's antennas, we design a MetaShield configuration that focuses the

incoming wave to the AP's receive aperture. In particular, we impose a radial phase gradient on the meta-atoms that provides a focus function, analogous to a lens. Moreover, we spatially place this function on the metasurface such that it aligns with the determined location, thereby maximally enhancing signals only from the intended transmitter.

(2) Directional interference mitigation via resonance-enabled attenuation. Other than the direction of the currently transmitting client, all other directions are potential sources of interference. To block such interferers, we configure MetaShield's meta-atoms to resonate in all directions other than that of the intended transmitter (which is focused). In particular, we configure meta-atoms to absorb the energy of incoming electromagnetic waves so that they cannot pass through the metasurface. This is realized via a single-mode resonance configuration of the meta-atoms that exhibits wide band power attenuation around the design frequency. Thus, even if the AP uses receive beam forming, MetaShield will protect it from receiving side lobe interference or interference outside of it's (potentially large) receive beamwidth.

AP-Controlled Temporal and Spatial Reconfigurability. To simultaneously realize multiple functions to different regions around the AP, we design MetaShield to spatially distribute different configurations over the surface. Moreover, the spatial configuration can be changed over time as different users are served and different functions are required.

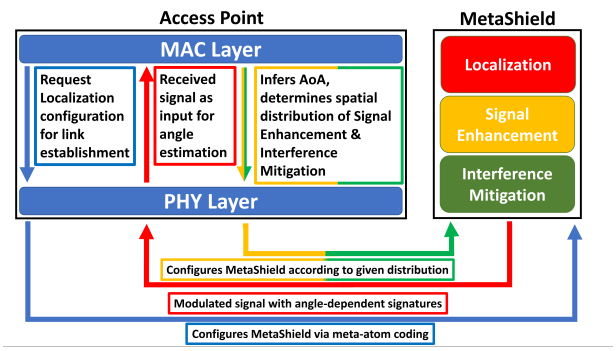

Figure 2: Control flow between the AP and MetaShield.

For example, during link establishment or if the client moves, MetaShield is configured to the localization configuration [8] to localize the client. This location information is then used by the AP to determine both the beamforming direction and the spatial distribution of focusing and blocking regions of MetaShield, along with other physical and MAC-layer requirements. For example, if the MAC layer control plane is associating a new client, MetaShield's localization configuration can be invoked. Finally, the AP is coupled to and controls MetaShield according to the determined spatial distribution of the functions. Figure 2 illustrates the control structure between the AP and MetaShield.

Finally, while we limit our study to MetaShield's uplink receive capabilities in this paper, MetaShield can also be configured for downlink transmission, e.g., to realize beamforming from the AP to clients, or beamfocusing if the client is in the nearfield.

3 DESIGN AND REGIONAL CONFIGURATION OF METASHIELD

In this section, we first provide the background principles for metasurfaces and how they can enable a wide range of functionalities that manipulate the wireless communication environment through their adjustable EM response. Then, we introduce the meta-atom geometry we adopt in our work, the C-Shaped Split Ring Resonator, and its physical and electromagnetic properties. Finally, we describe the design process for each configuration of MetaShield, i.e., Focuser Configuration for Signal Enhancement and Single-Mode Resonance Configuration for Interference Mitigation.

3.1 Metasurfaces and C-shaped Resonators

Metasurfaces are two-dimensional structures that enable sub-wavelength manipulation of the incident EM wavefront and can realize anomalous EM material properties, i.e., properties that cannot be attained by materials found in nature, such as negative permittivity and permeability [20]. Metasurfaces typically consist of many subwavelength-scale resonators, commonly named as meta-atoms, placed on a substrate. A meta-atom exhibits individual amplitude and phase responses that can be adjusted by manipulating its geometry [21]. Consequently, the EM response of a metasurface is engineered through the individual amplitude and phase responses of its many meta-atoms, as well as their relative placement on the surface.

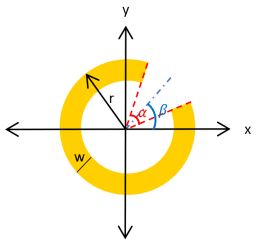

Figure 3: Geometric parameters of a CSRR.

We use the C-shaped Split Ring Resonator (CSRR) as the meta-atom geometry to design and experimentally evaluate MetaShield (Figure 3). CSRRs have strong interaction with EM waves in millimeter wave to sub-THz spectrum and its geometry allows simultaneous control of amplitude and phase [22, 23]. Furthermore, the simplicity of the geometry enables ease of design, enabling programmable CMOS implementations, e.g., [24]. The amplitude, phase, and polarization

responses of a CSRR meta-atom is determined by its geometric parameters: α is the opening angle, β is the orientation angle, r is the outer radius, w is the ring width.

3.2 Single-Mode Resonance Configuration

In this section, we describe our design of the Single-Mode Resonance configuration that suppresses unintended signals for the required regions of MetaShield. Moreover, because the receiver is polarization sensitive, the objective is to attenuate interfering signals in the same polarization as the receiver. Thus, to maximally suppress interference at the intended polarization, we configure meta-atoms in the desired regions of the metasurface to maximally resonate, i.e., to absorb or reflect incoming EM waves rather than letting them pass through the metasurface to the AP. To realize this idea, we determine the geometric parameters of the meta-atom that yield minimum transmission rate at the center frequency 150 GHz. For a horizontally polarized (x-polarized) input wave, there are distinct resonances depending on whether $\beta = 0°$ or 90°, which correspond to symmetric and anti-symmetric modes [22]. Consequently, we select the best attenuation performance over the parameters opening angle α, radius r, and for the two orientations. To do so, we conduct a finite-element-method parametric sweep of the parameters, i.e., for each parameter set, we use Maxwell's Equations to numerically compute the output response of the meta-atoms to an input plane wave with horizontal polarization. We set the ring width w to be proportional to the outer radius with a ratio of 1 to 3.

Over the search space, one geometry with 0° and one with 90° orientation (β) provide the lowest transmission rates, and are close in value to each other. We select the geometry with $\beta = 0°$, radius $r = 400\mu$m, and opening angle, $\alpha = 60°$ (figure describing simulation results can be found in [8]). For the horizontally polarized input wave, this geometry corresponds to a symmetric single mode resonance, which typically corresponds to a broader resonance bandwidth compared to $\beta = 90°$.

3.3 Focuser Configuration

Here, we describe the design process for the Focuser Configuration of MetaShield. We design a phase modulation that focuses the incident beam to the RX aperture and leverage the wide surface area of MetaShield in the near field of the AP at a known distance to enhance the reception of the intended signals.

In order to realize the same EM response as a focusing lens, a focusing metasurface must have a hyperboloidal phase distribution over its surface, which can be formulated as a function of the carrier frequency and the desired focal length via Fermat's principle [16]:

$$\Phi(\rho) - \Phi(0) = \frac{2\pi}{\lambda}(\sqrt{\rho^2 + f^2} - f) \quad (1)$$

where $\Phi(\rho)$ is the phase shift introduced at points located at distance ρ from the center of the metasurface, f is the focal length and λ is the wavelength. The focal length is determined by the separation length between MetaShield and the antennas of the AP it is affixed to, which is known pre-implementation, and we assign wavelength as 2 mm according to the carrier frequency 150 GHz. Note that required phase distribution for different carrier frequencies can easily be determined by modifying the wavelength in Equation (1) accordingly. Therefore, the AP can reconfigure MetaShield according to the current center frequency of different channels, as needed.

Since metasurfaces consist of discrete meta-atoms, we approximate Equation (1) by discretely sampling the function for the location of each meta-atom, and appropriately configure the meta-atom according to the corresponding value of function. An example realization is depicted in Figure 4a and 4b for a 60 mm focal length at 150 GHz. We realize this hyperboloidal phase distribution by selecting among one of eight meta-atom geometries with near-constant amplitude and a phase response that covers the entire [0,2π] range. Note that the outgoing focused beam is generated in the cross-polarization with respect to the incident wave, as [0,2π] phase control capability of CSRRs are shown in this regime [22]. Finally, we assign one of the eight geometries for every meta-atom over the surface according to the phase shift required at that meta-atom's placement, given by the hyperboloidal phase distribution. The resulting meta-atom placement for the 60 mm focuser is shown in Figure 4b.

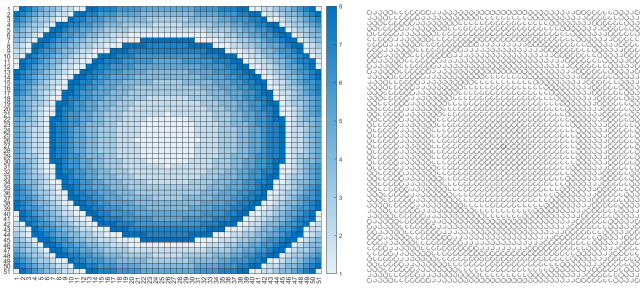

(a) Phase profile: 60 mm f & 150 GHz **(b) Meta-atom placement**

Figure 4: Focuser Configuration Design

4 IMPLEMENTATION AND OVER-THE-AIR EXPERIMENTS

In this section, we provide the performance analysis of MetaShield based on two different sets of experiments: Interference Mitigation and Signal Enhancement.

4.1 Fabrication of MetaShield

While MetaShield's reconfigurable, transmissive and conformal architecture is ambitious, the key architectural components have been demonstrated: a "reconfigurable transmissive" (including the control feed network) metasurface with GHz-rate switching speed is demonstrated in [24], and a curved metasurface is realized in [25], where the curvature is reported to affect the EM response minimally. Moreover, high transmissive efficiency is possible with new materials, e.g., transmissive metasurfaces with high aspect-ratio silicon micropillars were demonstrated to have up to 92% efficiency in [26]. Nonetheless, to the best of our knowledge, a metasurface architecture with all of the three features proposed for MetaShield has not been realized yet. Therefore, to experimentally analyze MetaShield and its individual configurations, we use multiple static metasurfaces and emulate the reconfigurable architecture.

For the fabrication of static metasurfaces, we adopted the hot-stamping technique [27]. This technique enables rapid and inexpensive production of metasurfaces functioning in the mmWave & THz range, enabling a faster and wider range of experimental analyses of different metasurface designs described in the previous section. The first step of metasurface fabrication via hot-stamping is to print the configuration, i.e. geometric layout of the designed meta-atoms, on a glossy paper with a toner-based office printer. Then, the paper is placed in between two sheets of plastic laminating pouch, with a layer of aluminum-based foil on top of the design. The pouch is laminated using an office laminator multiple times to yield a strong toner-aluminum bond resulted by the heat. Following the lamination, peeling off the top layer reveals the metallic resonators, in the geometry of the printed design, on top of the paper substrate. The flexibility of the paper substrate further enables the realization of the conformal structure of MetaShield by wrapping the substrate around a frame that surrounds the AP.

4.2 Interference Mitigation

Research Question. In this experiment, we evaluate the signal suppression performance of the Single-Mode Resonance configuration of MetaShield. As described in Section 2, this configuration is used to mitigate interference impinging on the AP from all unintended transmitters, e.g., clients in neighboring cells with side lobes. To evaluate the interference mitigation performance of this configuration, we first characterize the signal attenuation when the interferer is directly beamforming towards the AP and is aligned with the AP's main lobe. Realistically, an AP does not intentionally beamform towards an interferer, however, this is the worst case scenario for an AP, therefore we characterize this case to explore the worst case performance of the Single-Mode Resonance configuration. Second, since a practical case is the AP receiving interference from the side angles while beamforming towards an intended user, we evaluate the performance of the configuration at a range of angles around the RX beamforming direction. In both cases, we analyze the signal attenuation at neighboring frequencies as well as the design frequency 150 GHz, since communication established in this frequency region is likely to utilize wide bandwidth, consequently requiring stable interference mitigation over the entire band.

Experimental Setup. We fabricate an 80x80 mm planar metasurface with our Single-Mode Resonance Configuration using the hot-stamping technique. To correct for the fabrication inaccuracies introduced by hot-stamping, we fabricate multiple metasurfaces consisting of similar meta-atom geometries to the design in Section 3, and use the configuration with lowest transmission at 150 GHz, which corresponds to 450 μm radius and 50° opening angle. For data collection, we construct the setup shown in Figure 5, in which a single TX-RX pair and a rotational stage is used to collect the transmitted signal over the angle of arrival range [-18°,18°]. For signal generation, the TX and the RX are placed 30 cm away from each other, and are connected to the TeraMetrix T-Ray 5000 TDS-THz system, which generates wide band terahertz pulses. While the spectroscopy method facilitates the analysis of MetaShield's frequency response on a broad spectrum, the sub-microwatt transmitter limits the maximum experimental distance between the TX and RX. Nonetheless, wireless links established in the sub-THz region (210-240 GHz) extending to multi-kilometer distances have been shown in the literature [28]. Finally, we place the planar metasurface on the same rotation axis with the TX, normal to the direction of the wave vector, and collect the transmitted signal over the angle range. We repeat the process without the metasurface to determine the achieved attenuation.

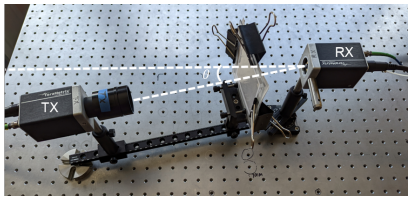

Figure 5: Single-Mode Resonance Configuration Setup.

Results. *RX-Aligned Interferer.* Figure 6a shows the signal transmission of the Single-Mode Resonance design at 0°, with a 100 GHz frequency range on the x-axis and transmitted power in dB, normalized with respect to the received power without the metasurface, on the y-axis. Recall that the meta-atom geometry in the design was configured to yield minimum transmission at the target frequency of 150 GHz. In Figure 6a, we observe that transmission is minimized

(and hence attenuation is maximized) at 150 GHz with -13.2 dB. For comparison, the suppression caused by the paper substrate alone is within 0.9 to 1.3 dB at the same angle. This shows that the design, even with a low-resolution fabrication technique, is able to cause significant signal suppression. In addition to the center frequency, transmission is below -9 dB for a bandwidth of 20 GHz, due to the wideband resonance of CSRR meta-atoms. Combined with the -13.2 dB transmission at the center frequency, this result shows that RX-aligned interferers within the 20 GHz band centered at 150 GHz are significantly suppressed, demonstrating the effectiveness of the design in the worst case.

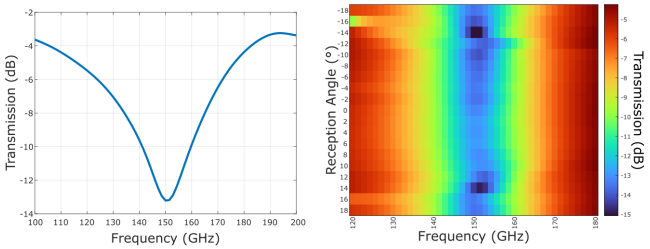

(a) RX-Aligned Interferer transmission spectrum. **(b) Transmission spectra at different angles of arrival.**

Figure 6: Signal transmission of MetaShield. (negative transmission corresponds to attenuation)

Side Angle Interferers. In practice, interferers will be angularly away from the receiver's direction of maximum SNR. Thus, here we study the signal suppression at a range of angles of arrival to evaluate the wide-angle interference mitigation performance of MetaShield. In Figure 6b, the x-axis shows a 60 GHz frequency range around 150 GHz and the y-axis shows the angle of arrival range [-18°,18°], and the color indicates the transmission in dB. Notice that at 150 GHz, the transmission is below -13 dB for all angles, with variations between -13 and -15 dB throughout the range. The variation within this 2 dB window can be explained by the noise power becoming more significant at side angles, where the difference between adjacent angles is noticeably higher. However, no performance degradation is observed at the side angles, with values close to the average -13.51 dB at the edges. Moreover, the transmission is below -9 dB for a 20 GHz band centered at 150 GHz throughout the angle range. Thus, the signals in the 140-160 GHz band from unintended directions are significantly suppressed, allowing the allocation of the band for intended transmission. Furthermore, the attenuation varies within a range of 0.8 dB at 140 GHz and 1.4 dB at 160 GHz, showing stable signal blocking performance at the edge frequencies, as well as the center frequency. Thus, Single-Mode Resonance design provides significant interference mitigation over a 20 GHz band for a broad angular range around the receiver, therefore safeguarding this band for a wide band intended link with low interference to be established at the desired angle.

Findings. By leveraging the symmetric mode resonance characteristics of the CSRR meta-atoms, the Single-Mode Resonance Configuration of MetaShield yields up to 15 dB suppression at the design frequency. Moreover, suppression can be realized over wide bandwidths with at least 9 dB suppression over 20 GHz. Lastly, suppression can be realized over wide angles that will subsequently protect the receiver from interferers in both its main and side lobes.

4.3 Signal Enhancement

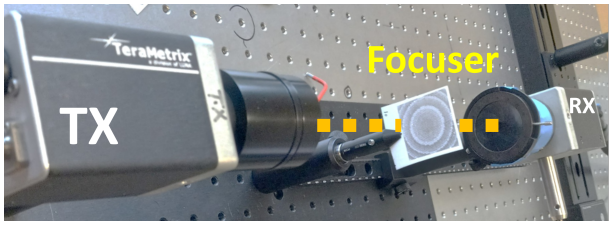

(a) Experimental Setup

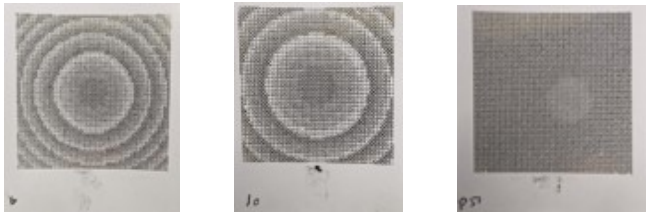

(b) 60 mm Focuser **(c) 100 mm Focuser** **(d) Beamformer**

Figure 7: Setup for Focuser Configuration.

Research Question. In this experiment, we study the signal enhancement performance of the Focuser Configuration of MetaShield, which is designed to enhance the intended transmission link. First, to evaluate its maximum signal enhancement capability, we study the SNR gain at the design frequency and focal length, with a beamformer metasurface as the baseline. Following the maximum performance, we expand our observation to a range of MS-to-RX distances to evaluate the robustness of the focal-length-specific design to possible mismatches in implementation, i.e., the model-based design sensitivity. Finally, we study the focusing bandwidth of the design to analyze its applicability to wideband links. While the phase distribution over the surface determined by Equation (1) depends on the wavelength, a communication link at this frequency region is desired to utilize a wide bandwidth, requiring consistent signal enhancement.

Experimental Setup. First, following the design principle explained in Section 3.3, we fabricate two focuser metasurfaces with focal lengths 60 mm and 100 mm to operate at 150

GHz, with a size of 51x51 meta-atoms (40x40 mm). By evaluating the design at two different focal lengths, we explore the ability of MetaShield to be deployed around receivers with varying dimensions. Second, we design a beamformer metasurface as a baseline. Since in our setup, the TX, MS, and RX are all aligned on the axis of propagation, i.e., broadside communication is performed, and the TX beam is highly directive, the beamformer metasurface has a constant zero phase gradient throughout the surface. To achieve such a phase gradient, we designed a single meta-atom geometry that provides maximum amplitude transmission at 150 GHz , and placed the same geometry into all of the cells in the 51x51 array. Finally, we set the RX to be in the cross-polarization to the TX as explained in Section 3.3, and use an iris piece at the RX side to set the aperture diameter to 5 mm for accurate observation of the focal point. We then collect the transmitted signal at a range of distances by moving the RX over the focal axis, with the beamformer, the 60 mm focuser, and the 100 mm focuser placed in between the TX and the RX separately (Figure 7).

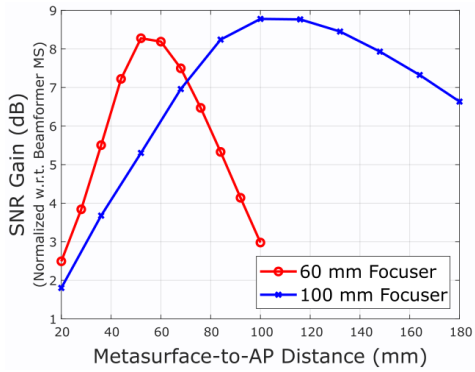

Figure 8: SNR Gain achieved by the focusers at 150 GHz.

Results. The SNR gain in the received signal achieved by the focuser design is shown in Figure 8. In this figure, the x-axis is the distance between the RX and metasurface, and the y-axis is the SNR gain in dB at 150 GHz, normalized with respect to the beamformer metasurface. The red and blue curves depict the enhancement achieved by the 60 mm and 100 mm focusers, respectively. A concave gain curve with a single peak can be observed clearly for both samples, with respective maximum enhancement values of 8.3 dB and 8.8 dB. Thus, both samples provide over 8 dB of SNR gain more than the beamformer at their respective focal length. Additionally, the maximum gain is observed at distances 52 mm and 100 mm respectively, corresponding to the empirical focal length values. Note that for the 60 mm focuser, the difference in gain between the theoretical and the empirical focal length is less than 0.1 dB. Furthermore, the maximum difference in the SNR gain between the theoretical focal length and an adjacent distance value is 0.8 dB and 0.54 dB for 60 mm focuser and 100 mm focuser, respectively. Compared to the maximum gain of 8.3 and 8.8 dB, these difference values show that the design is robust to small mismatches between the theoretical and empirical focal length at 150 GHz. Furthermore, such a mismatch can also be calibrated for by reconfiguring MetaShield in an online manner. In addition to providing significant enhancement at 150 GHz, the focusers exhibit a significantly wide band behavior with clear focal points over a 100 GHz range (the visualized results can be found in [8]). Furthermore, at 140 GHz and 160 GHz, the 60 mm focuser provides 8.4 and 7.4 dB gain at 60 mm, and the 100 mm focuser provides 9.8 and 7.6 dB gain, respectively. Thus, despite the focal length shift in adjacent frequencies as governed by Equation (1), the focuser design still provides over 7 dB gain at the designed focal length for a 20 GHz bandwidth. Therefore, we can conclude that the focusing configuration of MetaShield enables signal enhancement applications for a 20 GHz wide band communication link.

Findings. We adopted a near-field focuser design, enabled by the AP-coupled architecture of MetaShield, which demonstrated a clear enhancement of up to 8.8 dB in the SNR gain compared to the beamformer at the designed focal length and frequency. The small mismatch between the theoretical and experimental focal length for the 60 mm focuser is possibly a result of shrinkage during fabrication. As put forward by Equation (1), the phase distribution over a certain surface area determines the focal length, therefore any shrinkage in the surface area causes a sharper phase profile, resulting in a shorter empirical focal length. Despite the mismatch, the focuser still provided 8.2 dB gain at the theoretical focal length for 150 GHz. This can be attributed to the fact that the theoretical focal length for 150 GHz is the empirical focal length for a slightly higher frequency, and the CSRR meta-atoms have a wide band resonance behavior, which we previously showed in Figure 6a. In addition to the robustness to focal distance, the wide band resonance of the CSRR translates into a wide band focusing behavior, with focal points over a 100 GHz range and over 7 dB gain at a single focal point for a 20 GHz band around the design frequency.

5 CONCLUSION & FUTURE WORK

In this work, we proposed MetaShield, a multi-function metasurface affixed to and surrounding an AP, and is controlled by the AP to provide subwavelength scale amplitude and phase manipulation. We realized two functionalities over MetaShield by designing two meta-atom configurations: Single-Mode Resonance Configuration for Directional Interference Mitigation, and Focuser Configuration for Angle-Selective Signal Enhancement. Our experimental results demonstrate the effectiveness of the designed configurations, as well as the viability of providing different

functionalities concurrently over a single surface. Reconfigurable architecture of MetaShield is essential for its integration into wireless networks, therefore we envision to realize reconfigurable fabrication in the future. While we explored its uplink capabilities in this work, MetaShield's functionalities can also be applied to downlink communication with further optimization, e.g. integrating distance estimation for downlink beam focusing onto users in the environment.

6 ACKNOWLEDGMENTS

This research was supported by NSF grants CNS-2148132, CNS-2211618, CNS-1955075, CNS-1801865 and DOD: Army Research Laboratory grant W911NF-19-2-0269.

REFERENCES

[1] M. Renzo, A. Zappone, M. Debbah, M.-S. Alouini, C. Yuen, J. Rosny, and S. Tretyakov. Smart radio environments empowered by reconfigurable intelligent surfaces: How it works, state of research, and the road ahead. *IEEE Journal on Selected Areas in Communications*, 38(11):2450–2525,, 2020.

[2] Marco Di Renzo, Merouane Debbah, Dinh-Thuy Phan-Huy, Alessio Zappone, Mohamed-Slim Alouini, Chau Yuen, Vincenzo Sciancalepore, George C. Alexandropoulos, Jakob Hoydis, Haris Gacanin, and et al. Smart radio environments empowered by reconfigurable ai metasurfaces: An idea whose time has come. *EURASIP Journal on Wireless Communications and Networking*, 2019(1), 2019.

[3] Daisuke Kitayama, Yuto Hama, Kenta Goto, Kensuke Miyachi, Takeshi Motegi, and Osamu Kagaya. Transparent dynamic metasurface for a visually unaffected reconfigurable intelligent surface: Controlling transmission/reflection and making a window into an rf lens. *Optics Express*, 29(18):29292, 2021.

[4] Kun Qian, Lulu Yao, Xinyu Zhang, and Tse Nga Ng. Millimirror: 3d printed reflecting surface for millimeter-wave coverage expansion. MobiCom '22, page 15–28, New York, NY, USA, 2022. Association for Computing Machinery.

[5] Dianhan Xie, Xudong Wang, and Aimin Tang. Metasight: Localizing blocked rfid objects by modulating nlos signals via metasurfaces. MobiSys '22, page 504–516, New York, NY, USA, 2022. Association for Computing Machinery.

[6] Lili Chen, Wenjun Hu, Kyle Jamieson, Xiaojiang Chen, Dingyi Fang, and Jeremy Gummeson. Pushing the physical limits of iot devices with programmable metasurfaces, 2020.

[7] Z. Shaikhanov, F. Hassan, H. Guerboukha, D. Mittleman, and E. Knightly. Metasurface-in-the-middle attack: from theory to experiment. ACM WiSec, 2022-05.

[8] Burak Bilgin and Edward Knightly. Metashield: a multi-function apsurrounding metasurface. Master's thesis, Rice University, 2023.

[9] João Pedro Pavia, Vasco Velez, Renato Ferreira, Nuno Souto, Marco Ribeiro, João Silva, and Rui Dinis. Low complexity hybrid precoding designs for multiuser mmwave/thz ultra massive mimo systems. *Sensors*, 21(18), 2021.

[10] Muhammad Yasir Javed, Nuutti Tervo, Marko E. Leinonen, and Aarno Pärssinen. Wideband inter-beam interference cancellation for mmw/sub-thz phased arrays with squint. *IEEE Transactions on Vehicular Technology*, pages 1–13, 2023.

[11] Reza Barazideh, Omid Semiari, Solmaz Niknam, and Balasubramaniam Natarajan. Reinforcement learning for mitigating intermittent interference in terahertz communication networks, 2020.

[12] Naila Rubab, Shah Zeb, Aamir Mahmood, Syed Ali Hassan, Muhammad Ikram Ashraf, and Mikael Gidlund. Interference mitigation in ris-assisted 6g systems for indoor industrial iot networks. In *2022 IEEE 12th Sensor Array and Multichannel Signal Processing Workshop (SAM)*, pages 211–215, 2022.

[13] Huan Yi, Shi-Wei Qu, Bao-Jie Chen, Xue Bai, Kung Bo Ng, and Chi Hou Chan. Flat terahertz reflective focusing metasurface with scanning ability. *Scientific Reports*, 7(1), 2017.

[14] Wei Kou, Yaxin Zhang, Ting Chen, Ziqiang Yang, and Shixiong Liang. Multifunctional linear-polarized terahertz focusing metasurface. *Microwave and Optical Technology Letters*, 62(8):2721–2727, 2020.

[15] Dan Hu, Xinke Wang, Shengfei Feng, Jiasheng Ye, Wenfeng Sun, Qiang Kan, Peter J. Klar, and Yan Zhang. Ultrathin terahertz planar elements. *Advanced Optical Materials*, 1(2):186–191, 2013.

[16] Qiu Wang, Xueqian Zhang, Yuehong Xu, Zhen Tian, Jianqiang Gu, Weisheng Yue, Shuang Zhang, Jiaguang Han, and Weili Zhang. A broadband metasurface-based terahertz flat-lens array. *Advanced Optical Materials*, 3(6):779–785, 2015.

[17] Naeem Ullah, Weiguang Liu, Guocui Wang, Zongyuan Wang, Ata Ur Khalid, Bin Hu, Juan Liu, and Yan Zhang. Gate-controlled terahertz focusing based on graphene-loaded metasurface. *Optics Express*, 28(3):2789, 2020.

[18] Xuzheng Zhu, Yongzhi Cheng, Junpeng Fan, Fu Chen, Hui Luo, and Ling Wu. Switchable efficiency terahertz anomalous refraction and focusing based on graphene metasurface. *Diamond and Related Materials*, 121:108743, 2022.

[19] Quanlong Yang, Jianqiang Gu, Dongyang Wang, Xueqian Zhang, Zhen Tian, Chunmei Ouyang, Ranjan Singh, Jiaguang Han, and Weili Zhang. Efficient flat metasurface lens for terahertz imaging. *Opt. Express*, 22(21):25931–25939, Oct 2014.

[20] S.S. Bukhari, J.Y. Vardaxoglou, and W. Whittow. A metasurfaces review: Definitions and applications. *Applied Sciences*, 9(13):2727,, 2019.

[21] N. Yu and F. Capasso. Flat optics with designer metasurfaces. *Nature Materials*, 13(2):139–150,, 2014.

[22] X. Zhang, Z. Tian, W. Yue, J. Gu, S. Zhang, J. Han, and W. Zhang. Broadband terahertz wave deflection based on c-shape complex metamaterials with phase discontinuities. *Advanced Materials*, 25(33):4567–4572,, 2013.

[23] L. Liu, X. Zhang, M. Kenney, X. Su, N. Xu, C. Ouyang, Y. Shi, J. Han, W. Zhang, and S. Zhang. Broadband metasurfaces with simultaneous control of phase and amplitude. *Advanced Materials*, 26(29):5031–5036,, 2014.

[24] Suresh Venkatesh, Xuyang Lu, Hooman Saeidi, and Kaushik Sengupta. A high-speed programmable and scalable terahertz holographic metasurface based on tiled cmos chips. *Nature Electronics*, 3(12):785–793, 2020.

[25] Yaseman Shiri, Hichem Guerboukha, and Daniel M. Mittleman. Terahertz beam steering with curved metasurfaces. *Journal of Infrared, Millimeter, and Terahertz Waves*, May 2023.

[26] Zhuo Wang, Yao Yao, Weikang Pan, Haoyang Zhou, Yizhen Chen, Jing Lin, Jiaming Hao, Shiyi Xiao, Qiong He, Shulin Sun, and Lei Zhou. Bifunctional manipulation of terahertz waves with high-efficiency transmissive dielectric metasurfaces. *Advanced Science*, 10(4):2205499, 2023.

[27] H. Guerboukha, Y. Amarasinghe, R. Shrestha, A. Pizzuto, and D.M. Mittleman. High-volume rapid prototyping technique for terahertz metallic metasurfaces. *Optics Express*, 29(9):13806,, 2021.

[28] Priyangshu Sen, Jose V. Siles, Ngwe Thawdar, and Josep M. Jornet. Multi-kilometre and multi-gigabit-per-second sub-terahertz communications for wireless backhaul applications. *Nature Electronics*, 6(2):164–175, 2022.